Bioscience Nanotechnology

RESEARCH

Open Access

Ex vivo hemocompatibility and hemorheological evaluation of liposomal nanocarriers containing furosemide and blueberry extract

Victoria Judurcha[1,2], Ayelen M. Sosa[1,2,8,9], Analía I. Alet[3,5,6,10], Marcus V. Batista da Silva[3], Horacio V. Castellini[4], Bibiana D. Riquelme[3,5,6], Silvia del V. Alonso[1,2] and David Emanuel Ybarra[1,2,7,8*]

Abstract

Bovine mammary edema is a frequent clinical condition that impairs animal welfare and causes economic losses in livestock production, motivating the search for improved therapeutic strategies. In this work, liposomal nanocarriers were developed to incorporate Furosemide (Fr), a loop diuretic, and an anthocyanin-rich blueberry extract (BE), a natural antioxidant source. The antioxidant capacity of BE was confirmed by the DPPH assay, yielding an IC_{50} of 27 mg/mL, which was used to define the concentration employed for the liposomal formulation. The selected formulation exhibited a hydrodynamic diameter of 278.5 ± 9.2 nm, a polydispersity index of 0.28 ± 0.06, and a negative zeta potential, indicating the formation of nanoscale vesicles. Encapsulation efficiency analysis revealed moderate loading in single-compound systems (Fr: 51.12%; BE: 74.93%). However, in the co-loaded formulation, a marked decrease in encapsulation efficiency was observed (Fr: 0.8%; BE: 28.02%), indicating limited incorporation of Furosemide under the studied conditions. FT-IR analysis suggested interactions between the liposomal matrix and the incorporated compounds while preserving their main functional groups. However, BE-loaded liposomes did not exhibit detectable antioxidant activity under the tested conditions, likely due to limited accessibility of the encapsulated compounds to the DPPH radical and reduced effective concentrations in the liposomal formulations. Hemocompatibility studies using bovine red blood cells showed negligible hemolysis (< 5%) and no significant alterations compared to the negative control. Additionally, hemorheological evaluation indicated that the formulations did not adversely affect erythrocyte behavior. Overall, these results demonstrate that while liposomal systems provide a suitable platform for incorporating BE and evaluating physicochemical and hemocompatibility properties, the co-loading with Furosemide is markedly limited under the present conditions. These findings highlight the need to optimize formulation parameters further to achieve effective co-encapsulation in future studies.

Keywords Liposomes, Furosemide, Blueberry extract, Bovine red blood cells

*Correspondence:
David Emanuel Ybarra
david.ybarra@unahur.edu.ar
Full list of author information is available at the end of the article

Graphical Abstract

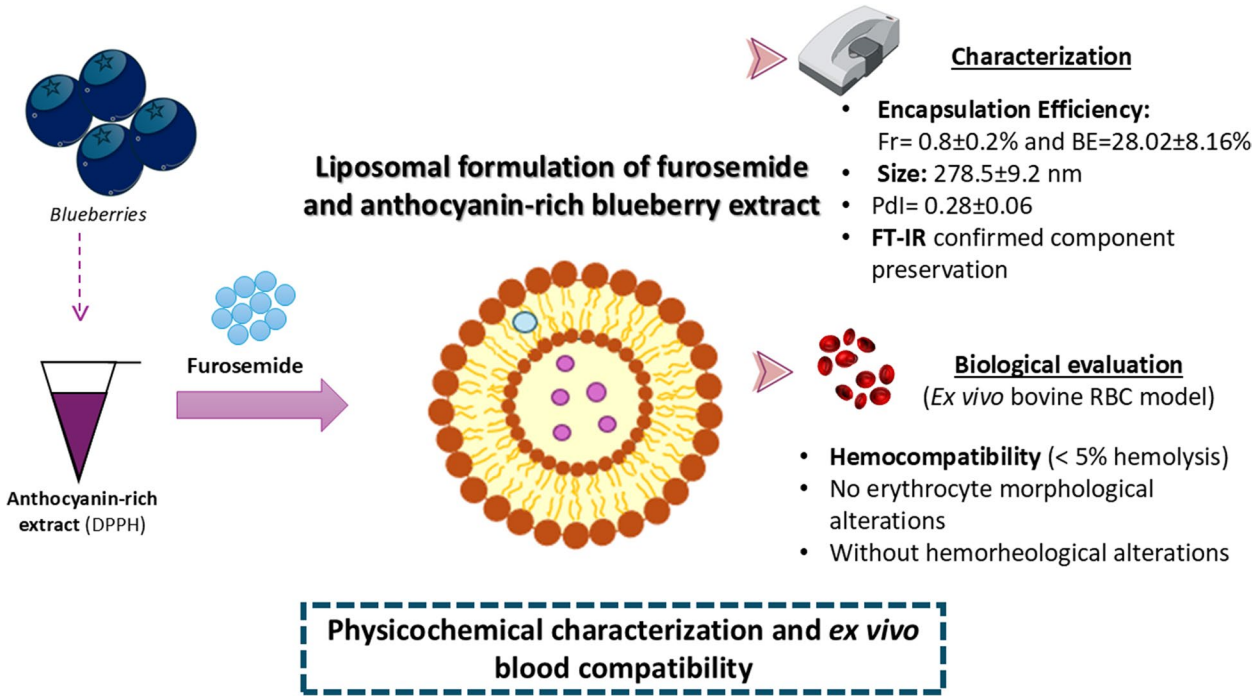

Introduction

Cattle farming is a vital economic activity that is essential to increasing meat and milk production worldwide. A dairy cow's welfare directly affects its productive capacity, as illness and metabolic energy are diverted from milk production, growth, and reproduction to the immune system [1]. As rural producers seek to increase animal production quickly, physiological and metabolic disorders occur more frequently in herds. Mammary edema is a common non-infectious peripartum disorder in dairy cows that significantly affects udder health and milk production [2, 3]. This condition is characterized by the accumulation of lymphatic fluid in the interstitial spaces of the mammary gland, leading to tissue swelling and discomfort [3]. Fluid accumulation in the udder tissue can compromise milk yield and increase susceptibility to secondary infections such as mastitis [4]. It has been reported that the prevalence of mammary edema affects a substantial proportion of dairy cows during the periparturient period, resulting in economic losses for the dairy industry [5].

Furosemide (Fr) is commonly used in veterinary practice for the treatment of edematous conditions. It is a potent loop diuretic widely employed in both human and veterinary medicine due to its ability to promote rapid diuresis and reduce fluid accumulation [6]. The product is administered via parenteral route, subcutaneous injection, intravenous, intramuscular, or intravenous [7]. However, its bioavailability is approximately 50–70%, and 60–70% of the dose is eliminated as an unchanged drug, primarily through secretion in the proximal tubule.

In addition to fluid accumulation, inflammatory processes associated with tissue edema may promote the generation of reactive oxygen species, potentially contributing to oxidative stress and tissue damage [8, 9]. Antioxidants are substances present in low concentration relative to the oxidizable molecule that delay or prevent the oxidation of this substrate [10]. Blueberries (*Vaccinium* spp.) are a rich natural source of flavonoids. These compounds have a high antioxidant power due to anthocyanins, a family of polyphenolic compounds synthesized by plants as secondary metabolites [11]. Interest in anthocyanin pigments has intensified due to their pharmacological and therapeutic properties [12]. It is known that they exert therapeutic effects, including reducing coronary disease, anticancer, antitumor, anti-inflammatory, and antidiabetic effects [13, 14]. In addition to their antioxidant capacity, anthocyanins have been reported to modulate inflammatory responses and oxidative stress in different biological systems. Since inflammatory

processes associated with tissue edema may promote the generation of reactive oxygen species, antioxidant compounds could potentially contribute to reducing oxidative damage in affected tissues [15, 16].

The application of nanotechnology in veterinary medicine, as in livestock farming, is relatively new, and in the last decade, it has received more attention due to its promise to enhance nutrition through multiple applications and products [17, 18]. In this sense, liposomes offer many advantages as drug carriers in preclinical and clinical trials [19]. Liposomes have been explored as versatile drug and gene delivery, enzymes or protein delivery, vaccines, and photodynamic therapy in biomedical applications [20–22]. Liposomes are colloidal spherical structures formed by the self-assembly of amphiphilic lipid molecules in solutions, such as phospholipids [23]. This structure allows the capacity to carry and deliver molecules with different solubilities. For example, hydrophilic molecules can integrate into the internal aqueous core of the liposomes. In the case of hydrophobic molecules, molecules can be delivered into the lipid bilayer. Finally, amphiphilic molecules could be internalized at the water/lipid bilayer interface [22]. Hence, liposomes could be proposed as a delivery system for Furosemide, allowing for better bioavailability and pharmacokinetic profile at the site of interest. This therapeutic combination strategy and the improvement of bioavailability through liposomal systems are principles that are applied in the formulation proposed in this work.

From a formulation perspective, the simultaneous administration of Furosemide and antioxidant compounds from blueberry extract presents several physicochemical and pharmacokinetic challenges. Furosemide has limited aqueous solubility at physiological pH and a relatively short systemic half-life due to its rapid renal elimination, which can restrict its therapeutic persistence at the target site [24, 25]. Conversely, anthocyanins, the main bioactive compounds in blueberry extract, are highly hydrophilic and chemically unstable under physiological conditions, being susceptible to oxidative degradation, pH-dependent structural transformations, and enzymatic metabolism [13, 26]. These characteristics can significantly reduce their biological activity in vivo. Liposomal nanocarriers represent a suitable strategy to overcome these limitations thanks to their unique architecture, composed of a phospholipid bilayer surrounding an aqueous core, which allows the encapsulation of molecules with different physicochemical properties within a single delivery system [27–29]. In this context, hydrophilic anthocyanins can be incorporated into the internal aqueous compartment, while amphiphilic molecules, such as Furosemide, can associate with the lipid bilayer. Furthermore, liposomal encapsulation can improve the physicochemical stability of labile compounds, modulate drug release kinetics, and potentially enhance biodistribution by promoting nanoparticle accumulation in inflamed or edematous tissues characterized by increased vascular permeability [30–32]. Therefore, the coencapsulation of Furosemide and antioxidant phytochemicals within liposomal nanocarriers may represent a promising strategy for combining diuretic and antioxidant therapeutic mechanisms on a single biocompatible platform.

To explore this concept, liposomal nanocarriers were proposed as a platform capable of simultaneously incorporating compounds with different physicochemical properties. Liposomes are particularly attractive systems because they can encapsulate both hydrophilic and lipophilic molecules, enabling the co-delivery of pharmacologically complementary agents within a single nanoscale carrier.

In this context, Fr was selected as the primary therapeutic agent due to its well-established diuretic activity and its common use in the treatment of bovine edema. Blueberry extract, rich in anthocyanins with antioxidant properties, was incorporated as a complementary component intended to counteract oxidative stress potentially associated with inflammatory processes occurring in edematous tissues.

So, the hypothesis of this study is that the co-encapsulation of Furosemide and antioxidant compounds from blueberry extract (BE) within liposomal nanocarriers may provide a biocompatible formulation capable of combining diuretic and antioxidant functionalities. Therefore, the aim of this work was to develop and characterize liposomal formulations co-loaded with Furosemide and blueberry extract and to evaluate their ex vivo hemocompatibility and hemorheological behavior using bovine red blood cells as a preliminary biological model.

Materials and methods

Materials

Blueberries (*Vaccinium myrtillus*) sourced from Entre Ríos, Argentina. The reagent 2,2-diphenyl-1-picrylhydrazyl (DPPH) and Furosemide (molecular weight = 330.74 g/mol) were purchased from Sigma-Aldrich (Merck, Argentina). Bunge Argentina donated Soy phosphatidylcholine (SPC), and S.A. Stearic acid (SA) was purchased from Vitalquim, Argentina. Cellulose filters with a pore size of 0.4 µm were from Sartorius. Sephadex G-75 was purchased from Sigma-Aldrich (Merck, Argentina). Sodic Heparin was from Duncan Laboratories, Argentina. Bovine blood was donated from Cooperativa Subpga Slaughterhouse (Berazategui, B1884HEH, Buenos Aires Province, Argentina). The ethanol used was of pharmaceutical grade. Other solvents (methanol, chloroform) were of analytical grade.

Extraction of blueberry extract enriched with anthocyanins

Blueberries (*Vaccinium myrtillus*) were stored at −18 °C until use. Blueberry extract was obtained by solid–liquid extraction following the method described by Nicolas GM et al. (2023) [33]. After solvent removal, the resulting blueberry extract (BE), rich in anthocyanins, was weighed, and the extraction yield was calculated using Eq. 1. The dried extract was stored at 4 °C wrapped in aluminum foil to protect it from light.

$$\%\text{Efficiency} = \frac{mass\ of\ blueberry\ extract}{mass\ of\ blueberries} \times 100 \quad (1)$$

Determination of the antioxidant capacity of blueberry extract

The antioxidant capacity was determined as informed by Franceschinis et al. (2023), using the 2,2-diphenyl-1-picrylhydrazyl (DPPH) radical test [34]. A solution of BE, rich in anthocyanins, was prepared in water at a final concentration of 102.4 mg/ml, and serial dilutions were made. The range of concentrations tested was 0.8–102.4 mg/ml ($n=4$), and measurements were repeated three times with different batches of blueberry extract on other days. Absorbance at 517 nm was measured using Cytation 5 (Thermofisher, USA). The DPPH radical scavenging activity was calculated using the following equation: [35]

$$\%\text{Inhibition} = \frac{Ac - As}{Ac} \times 100 \quad (2)$$

where Ac is the absorbance at 517 nm from the control sample, and As is the absorbance at 517 nm of the sample.

Preparation of the liposomal formulation

Soy phosphatidylcholine (SPC) was used as the main structural phospholipid to form the bilayer matrix of the vesicles. Stearic acid (SA) was incorporated as a co-lipid to modulate bilayer packing and surface properties, thereby improving the structural stability of the liposomal system. The SPC:SA molar ratio (1:0.25) was selected based on previous optimization studies of our research group [36]. However, this method was employed with some modifications. The molar ratio mentioned above was mixed with 4 mL of chloroform to obtain a final lipid concentration of 25 mM. After the lipidic film formed, the vesicles were rehydrated in aqueous solvents. These aqueous media consisted of 10 mM phosphate-buffered saline (PBS), pH 7.4, and osmolality 300 mOsm/L, or blueberry extract rich in anthocyanins (BE) solubilized in PBS at its IC50 ([BE] = 26.6 mg/mL). PBS was used to hydrate the lipid film because of its physiological pH and ionic strength, which provide a suitable environment for the self-assembly of phospholipids into stable liposomal vesicles. After reconstitution in the aqueous medium, the flask was mixed using a ZX3 Vortex Stirrer (Velp Scientifica, Italia) mixer at maximum speed (3000 rpm) to facilitate the detachment and dispersion of the lipid film. Subsequently, the sample was sonicated in a TESTLAB ultrasonic bath for 30 min at 30 °C at 40 kHz to reduce vesicle size. The liposomal suspension was filtered using a Minisart Sartorius syringe filter (0.4 µm) and stored at 4 °C until use. The liposomes containing Furosemide were prepared as described previously. In this case, the 20 mg/ml stock of Fr in methanol was added to the lipid mixture before the evaporation step. For clarity, all formulations are identified according to the nomenclature summarized in Table 1.

Optimization criteria guided the selection of liposomal formulations aimed at achieving the lowest possible hydrodynamic diameter and a low polydispersity index (PdI), indicative of a homogeneous size distribution. To this aim, different L:BE:Fr ratios were evaluated, varying the amount of furosemide from 1:0:0.25 up to 1:0.25:0.25.

Determination of encapsulation efficiency and quantification of encapsulated compounds

The encapsulation efficiency (EE%) of furosemide and blueberry extract in liposomal formulations was determined by separating the unencapsulated compounds by size-exclusion chromatography (SEC) using a column packed with Sephadex G-75, a method adopted by Fry et al. [37]. SEC columns were assembled using an ad hoc system. Sephadex G-75 was packed into 3 mL Euromix syringes (EURO SWISS S.A., Argentina), using glass wool at the base as a support filter. The syringe dimensions were approximately 12 cm in total length with an internal diameter of 9 mm. These dimensions correspond to an estimated bed volume of 3 mL. The column was then dried by centrifugation at 3000 rpm for 15 min. Briefly, the liposomal suspensions were loaded onto an SEC column and eluted by centrifugation (3000 rpm for 15 min) to isolate the vesicular fraction of the free (unencapsulated) compounds. The resulting liposomal fraction was dispersed by dilution (1:10) in absolute ethanol to ensure complete vesicle rupture and release of the associated compounds. The resulting mixture was centrifuged at 15,000 rpm for 15 min, and the supernatant was collected for analysis.

The concentration of BE was determined by fluorescence spectroscopy using a SCINCO S2 fluorometer (SCINCO Co., Ltd., Seoul, Republic of Korea). The calibration curve constructed from the stock extract ranges from 0.4 to 1.6 mg/ml ($n=5$). Quantification was based on the area under the emission curve (AUC), as described by the equation AUC = 120,861 × BE − 26,281

($R^2 = 0.98$). The calibration curve for furosemide (Absorbance = 0.006294 × Fr + 0.03216; $R^2 = 0.99$) was determined by UV–Vis spectrophotometry using a Nanodrop-1000 UV–Vis spectrophotometer (Thermo Fisher Scientific, USA) in the range of 2.5 to 100 µg/ml ($n = 5$).

Encapsulation efficiency (EE%) was calculated as the percentage of compound associated with the liposomal fraction relative to the initial amount used in formulation.

Spectroscopic characterizations

UV–visible absorbance measurements

UV–visible spectra were acquired using a Nanodrop-1000 UV–visible spectrophotometer (Thermo Fisher Scientific, USA) over 220–600 nm with a resolution of 3 nm.

Fluorescence emission measurements

Fluorescence spectra were recorded using the SCINCO S2 fluorometer (SCINCO Co., Ltd., Seoul, Republic of Korea). The parameters employed varied depending on the type of sample under analysis.

For samples containing blueberry extract, a slit width of 2.5 nm was utilized, with an excitation wavelength of 300 nm, and emission was detected in the range of 310–560 nm. In contrast, for samples containing Furosemide, the slit width was 5 nm, excitation occurred at 280 nm, and the emission range was 300–550 nm.

Fourier transform infrared spectroscopy

In Fourier Transform Infrared Spectroscopy (FTIR), 20 µL of each sample was placed onto the Nicolet 8700 FTIR Spectrophotometer (Thermo Fisher Scientific, USA) equipped with an Attenuated Total Reflectance (ATR) accessory. The aqueous solvent was evaporated using a hot air gun to remove water, and measurements were taken. Spectra were collected within the range of 4000–400 cm^{-1}. Finally, spectra were processed using IRsolution 1.5 software.

Hydrodynamic size and zeta-potential measurements by dynamic light scattering

The particle size was estimated using Dynamic Light Scattering (DLS). The temperature of the analysis was carried out at 25 ± 0.1 °C with a Zetasizer Advance Lab instrument from Malvern Panalytical (Malvern, UK). This instrument has an avalanche photodiode detector and a He–Ne laser with 4 mW at λ = 633 nm. Each formulation was analyzed five times.

To measure the zeta potential, all formulations were analyzed in triplicate at a temperature of 25 ± 0.1 °C using a Zetasizer Pro Blue instrument from Malvern Panalytical Ltd. (Malvern, UK). Data collection and analysis were performed with ZS Xplorer software (version 3.2.2.5, Malvern Panalytical Ltd., Malvern, UK).

Table 1 Formulation composition and nomenclature of the liposomal systems evaluated in this study

Sample	Composition			
	SPC	SA	Fr	BE
L	1	0.25	—	—
L:Fr	1	0.25	0.06	—
L:BE	1	0.25	—	0.9
L:BE:Fr	1	0.25	0.06	0.9

Interaction with bovine red blood cells

Blood sample collection and red blood cell isolation

Bovine blood was obtained from animals slaughtered for human consumption at Frigorífico Cooperativa Subpga (B1884HEH, Berazategui Oeste, Argentina). No live animals were used in this study. Blood samples were collected immediately after death by carotid puncture (< 2 h postmortem). For hemolysis studies, blood was collected in sterile heparinized (50 U/mL) tubes. For rheological studies, blood was fractionated in tubes with EDTAK3, also as an anticoagulant. Samples were transported to the laboratory at 4 °C and processed immediately upon arrival. Whole blood was centrifuged at 2000 × g for 15 min at 4 °C to remove plasma. The erythrocyte fraction was resuspended in phosphate-buffered saline (PBS) to obtain bovine red blood cells (bRBCs), which were used for subsequent hemocompatibility, morphological, and hemorheological analyses.

Hemocompatibility and morphological analysis

Hemocompatibility was assessed by hemolysis assays using bRBCs incubated with different formulations. Four concentrations of each component (liposomes, blueberry extract, and furosemide) were evaluated by serial dilution in PBS. The tested concentration ranges were 25–3.1 mM for L, 26.6–3.4 mg/mL for BE, and 1.5–0.2 mM for Fr. Samples were incubated at 37 °C for 24 h [38]. Hemoglobin release was quantified spectrophotometrically at 414 nm (Soret band) using a NanoDrop 1000 (Thermo Fisher Scientific, USA). Absorbance values were normalized to the positive control (CTR+), consisting of erythrocytes treated with 2% sodium dodecyl sulfate (SDS), defined as 100% hemolysis. Experiments were performed using two independent biological replicates (different animals), each with three technical replicates per condition (n = 6 total), to account for biological variability.

For morphological analysis, samples exhibiting hemolysis below 5% were selected. After incubation, cells were centrifuged and resuspended in PBS. A 5 µL aliquot was used to prepare blood smears, which were fixed in cold methanol (3 min) and stained with Giemsa solution (1:10 dilution). Slides were washed, air-dried, and examined

under an optical microscope (Cytation 5, Thermo Fisher Scientific, USA), and microphotographs were acquired in brightfield mode.

Hemorheological analysis and erythrocyte integrity assessment

For hemorheological studies, bRBC suspensions obtained as described above were used. Erythrocytes were resuspended in PBS (1:1, v/v) and subsequently mixed in equal volume with each treatment solution (L, L:BE, L:Fr, L:BE:Fr, and BE). A control sample was prepared using PBS. Prior to hemorheological measurements, erythrocyte suspensions were evaluated to confirm cellular integrity under native (unstained) conditions, ensuring that subsequent viscoelastic measurements were not affected by pre-existing membrane damage. Bovine red blood cells were suspended in autologous plasma at 0.25% v/v and observed in an inverted microscope (Union, Japan) with an attached digital camera [39, 40]. Five images of each bRBC sample were recorded to analyze the possible alterations in cell morphology.

Hemorheological measurements were performed using a custom-built erythrocyte rheometer based on a previously described patented design (Patent AR2013P102129) [41–44]. The instrument is specifically designed to evaluate the rheological behavior of erythrocyte suspensions by analyzing their response to controlled mechanical stress, enabling the determination of viscoelastic and deformability-related parameters. The system operates via laser diffraction and allows the determination of viscoelastic parameters of erythrocytes under both steady and dynamic conditions. These analyses were conducted to evaluate potential changes in membrane viscoelasticity induced by the different formulations. The viscoelastic parameters of the erythrocyte membrane obtained in the steady regime were:

- DI: deformability index of the erythrocyte membrane
- μ: elastic modulus of the erythrocyte membrane
- ηm: surface viscosity of the erythrocyte membrane

A volume of 100 μL of each bRBC sample (control or treated) was poured into 4.5 mL of a PVP solution for these determinations. This solution was prepared with polyvinyl-pyrrolidone (PVP360®, Sigma-Aldrich, Merck Argentina) at 5% (w/v) in PBS and had a viscosity of 22 cp at 25 °C. For each treatment, the data were obtained by quintuplicate.

Statistical analysis

Results were expressed as mean ± standard deviation. Statistical analysis was performed using GraphPad Prism 8. One-way ANOVA was applied where appropriate, followed by Dunnett's test for comparisons against the control and Tukey's test for multiple pairwise comparisons. Rheological data were analyzed using Student's t-test (Scientific Python). Differences were considered statistically significant at $p < 0.05$.

Results and discussion

Spectroscopic characterization of BE

The initial mass of blueberries was 48.9 g. After extraction, 6.18 g of BE were obtained. Macroscopically, the resulting film exhibited a dark red coloration. According to Eq. 1, the yield was calculated to be 12.64%. In the measured batch's UV–visible spectrum (Fig. 1A), two peaks were detected: one in the UV region from 250 to 280 nm and another in the visible region corresponding to 500–545 nm broadband. These signals are characteristic of anthocyanins and have been previously observed in other plant raw materials, such as fruits, juices, wines, and flowers [45]. The dependence of absorbance intensity on increasing BE concentration was observed. In the case of the first band (250–280 nm), absorption is associated with substituents of anthocyanin due to the aromatic chromophore group with hydroxyl and methoxy substituents. The broadband with the maximum absorption peak at 520 nm is due to the flavylium ion [46]. This ion has many conjugated double bonds, allowing absorption in the visible region of the spectrum and giving the characteristic red-blue color of anthocyanins.

Different concentrations of BE were analyzed by fluorescence spectroscopy (Fig. 1B). Excitation was at 300 nm, as this peak was the most significant in the UV, and detection was 310–560 nm. The BE showed a maximum fluorescence emission peak at 385 nm. This emission is due to the presence of aromatic groups in the anthocyanins. It is known that the phenolate ion and the cyanidin group absorb between 310 and 400 nm [47]. The results showed an increase in emission concentration dependent on 3.2 mg/ml. However, emissions decreased at 6.4 mg/ml and 12.8 mg/ml, which could result from a quenching effect at high concentrations, as more available molecules or the solvent (distilled water) interact, decreasing emissions.

In Fig. 1C, the FT-IR spectra are shown. Various characteristic signals corresponding to the vibrational modes present in anthocyanins were detected. The peak at 3350 cm^{-1} was attributed to hydroxyl groups, both free and bonded to other atoms. The hydroxyacetone shows a band between 3500 and 3200 cm^{-1}, indicating the presence of this functional group, characteristic of a possible anthocyanin structure. The peak at 1630 cm^{-1}, found between 1550 and 1650 cm^{-1}, was assigned to aromatic

rings with conjugated double bonds (C=C), which are responsible for the visible color of anthocyanins. The peak at 1000 cm^{-1} is due to the stretching of the C-O and C–C bonds.

Free radical inhibition assay by DPPH

Regarding the results of DPPH-mediated free radical inhibition, decreasing concentrations of BE were tested (Fig. 2A). Although concentrations in the 0.8–102.4 mg/ml range were tested, the technique linearly depends on the concentration range between 3.2 mg/ml and 51.2 mg/ml. A plateau was observed at higher concentrations, suggesting that the method loses sensitivity as the proportional response to sample concentration is no longer maintained.

Figure 2B plots a linear regression using the average DPPH radical scavenging inhibition percentages. The equation obtained for the curve was used to determine the antioxidant concentration required to reduce the initial DPPH radical concentration by 50% (IC50). The result obtained after applying linear regression was 26.6 mg/mL; this percentage of inhibition is similar to that reported by Giordano Maffioly et al. [33].

The inclusion of natural extracts in liposomal systems, such as blueberry extract, is often hypothesized to preserve their biological activity, depending on factors such as encapsulation efficiency, localization within the vesicle, and interactions with the lipid bilayer. For instance, Bahramabadi et al. (2024) reported the preservation of antibacterial activity in liposome-encapsulated rocket seed essential oil [48], supporting the potential of liposomal systems to maintain the functionality of bioactive compounds.

However, this behavior is not universal and must be experimentally verified for each system. Therefore, in the next section, the effect of BE incorporation into liposomal formulations on antioxidant activity is evaluated. In line with this, the antioxidant activity of BE-loaded liposomes was experimentally assessed and presented in the next section.

Obtaining and characterization of liposomal formulations

The physicochemical characterization of the liposomal formulations is summarized in Table 2, including hydrodynamic diameter, polydispersity index, zeta potential, and encapsulation efficiency (%EE) of both Furosemide and blueberry extract. The selection of liposomal formulations was guided by optimization criteria aimed at minimizing the hydrodynamic diameter and achieving a low polydispersity index (PdI), thereby favoring a more homogeneous vesicle population. Different L:BE:Fr ratios were evaluated, varying the proportion of Furosemide from 1:0.9:0.0 to 1:0.9:0.06 (or 2.5 to 10 mg of Fr).

Encapsulation efficiency (%EE) analysis revealed significant differences across liposomal systems. In single-loaded formulations, BE exhibited a relatively high encapsulation efficiency (74.93%), whereas Furosemide showed moderate incorporation (51.12%). These results are consistent with the physicochemical properties of both compounds: anthocyanins are highly hydrophilic and preferentially partition into the aqueous core of liposomes, whereas Furosemide, due to its amphiphilic nature, may distribute between the aqueous phase and the lipid bilayer.

In contrast, the co-loaded formulation (L:BE:Fr) showed a low encapsulation efficiency observed for furosemide in the co-loading system (0.8%) highlights a limitation of the co-formulation. This suggests that the system would not be suitable for the co-administration of both compounds. In comparison, BE encapsulation was also reduced (28.02%) compared to the single-loaded system. This behavior could be due to partitioning phenomena and the limited affinity of Furosemide for the selected lipid composition. Therefore, further optimization would

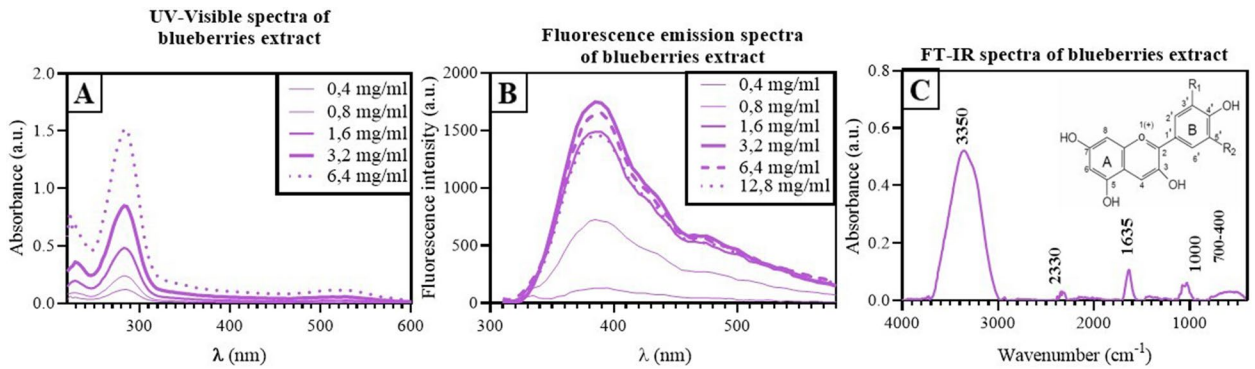

Fig. 1 Spectroscopic characterization of anthocyanin-rich blueberry extract. Different concentrations of BE were measured by (**A**) UV–visible spectroscopy, (**B**) fluorescence emission spectroscopy, and (**C**) the FT-IR spectrum is shown

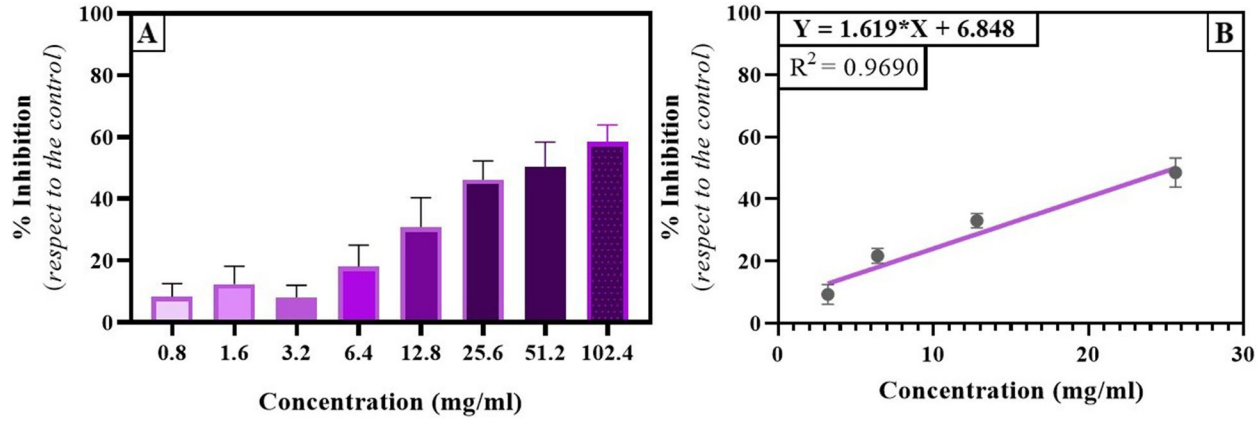

Fig. 2 Free radical inhibition by DPPH of BE. **A** Concentration vs. inhibition percentage graph. **B** Free radical inhibition curve as a function of concentration within the linear inhibition range. The linear range was established between 3.2 and 25.6 mg/ml

be required to improve drug incorporation. Such effects have been described in multicomponent liposomal systems, where compounds with different solubility profiles compete for distinct microenvironments within the vesicle.

Liposomes composed solely of phospholipids (L) had an average diameter of 259.3 ± 2.2 nm with a PdI of 0.31 ± 0.1. The incorporation of Furosemide (L:Fr) slightly reduced the average hydrodynamic diameter to 238.8 ± 9.1 nm, while maintaining a similar polydispersity index (0.31 ± 0.1). Conversely, liposomes with blueberry extract (L:BE) showed a significant ($p < 0.1$) increase in particle size (286.0 ± 22.7 nm) and a slightly wider size distribution (PdI = 0.34 ± 0.1). The complete formulation with both bioactive components (L:BE:Fr) exhibited an average hydrodynamic diameter of 278.5 ± 9.2 nm with a lower PdI value (0.28 ± 0.05), indicating a relatively homogeneous vesicle population. Regarding L:BE:Fr, the hydrodynamic size has shown a significant increase ($p < 0.01$) compared to L:Fr. According to the size distributions (Fig. 3), the smaller signals observed at larger sizes (e.g., ~ 10,000 nm) likely correspond to a small aggregate population that may contribute disproportionately to light scattering intensity due to their larger size, despite representing a negligible fraction of the sample. However, the Number percent distributions (Fig. 3B) confirm the formation of monomodal populations and correlate with the obtained PdI values.

Overall, PdI values below 0.35 indicate the formation of predominantly unimodal liposomal populations with acceptable size homogeneity. The combined formulation (L:BE:Fr) exhibited the lowest PdI value among the tested systems, with a PdI of 0.28 ± 0.05, suggesting a relatively homogeneous vesicle population. This behavior may be associated with interactions between the encapsulated compounds and the phospholipid bilayer that help stabilize the liposomal structure. Polyphenolic compounds, such as anthocyanins, have been reported to interact with lipid membranes via hydrogen bonding and polar interactions at the lipid–water interface, potentially influencing membrane packing and interfacial organization [47]. In parallel, amphiphilic

Table 2 Physicochemical characterization of liposomal formulations, including hydrodynamic diameter (Z-average), polydispersity index (PdI), zeta potential, and encapsulation efficiency (%EE) of Fr and BE. The values were shown as means ± SD ($n = 5$). Statistical analysis was performed using one-way ANOVA followed by Tukey's post hoc multiple comparisons test for Z-average and Z-potential measurements. Significant differences are indicated by superscript letters as follows: a–c denote comparisons versus L (empty liposomes) at different significance levels ($p < 0.05$, $p < 0.001$, and $p < 0.0001$, respectively); d indicates comparison versus L:Fr ($p < 0.01$); and e indicates comparison versus L:BE ($p < 0.0001$)

Sample	%EE		Z-average (nm)	PdI	Z-Potential (mV)
	Fr (%)	BE (%)			
L	—	—	259.3 ± 2.2	0.31 ± 0.1	−43.46 ± 0.04
L:Fr	51.12 ± 0.63	—	238.8 ± 9.1	0.31 ± 0.1	−36.11 ± 0.50 [b]
L:BE	—	74.93 ± 8.28	286.0 ± 22.7 [a]	0.34 ± 0.1	−46.25 ± 1.29
L:BE:Fr	0.8 ± 0.2	28.02 ± 8.16	278.5 ± 9.2 [d]	0.28 ± 0.05	−33.33 ± 2.40 [c,e]

molecules such as Furosemide may associate with the phospholipid bilayer, affecting lipid packing and membrane curvature [48]. The simultaneous presence of both compounds could therefore promote a more balanced organization within the liposomal structure, contributing to the formation of vesicles with narrower size distributions.

The zeta potential of the liposomal formulations was reported, yielding negative values ranging from approximately −33 mV to −46 mV, suggesting electrostatic stabilization and reduced aggregation. This negative charge can be attributed to the lipid composition of the system, particularly the presence of soybean phosphatidylcholine (SPC) and stearic acid, both of which contribute to the net negative surface potential under the experimental conditions [49] Interestingly, the magnitude of the zeta potential varied depending on the encapsulated components. The L:BE formulation exhibited the most negative value (−46.25 mV), which may be associated with the presence of phenolic compounds from the extract interacting at or near the lipid–water interface. In contrast, the co-loaded system (L:BE:Fr) showed a less negative zeta potential (−33.33 mV), suggesting partial screening or reorganization of surface charge in the presence of both compounds. This reduction in surface charge magnitude may also contribute to the observed decrease in encapsulation efficiency, as changes in interfacial properties can affect vesicle formation and stability.

On the one hand, Fr would interact with the lipid hydrocarbon chains inside the bilayer. On the other hand, and in conjunction with those mentioned above, the hydrophilic polyphenols of BE in the aqueous core or by interaction with the liposomal surface would synergistically stabilize the liposomal structure. This would lead to greater uniformity in size due to interactions between the present molecules and the liposome components. Overall, these results indicate that while both compounds can be successfully incorporated into liposomal systems individually, their simultaneous encapsulation presents formulation challenges that impact loading efficiency and interfacial properties. However, the charged formulation of both compounds maintains a nanoscale size, acceptable polydispersity, and sufficient surface charge, ensuring colloidal stability and supporting its viability as a co-delivery platform; however, further optimization may be needed to improve encapsulation performance.

In the UV–visible spectrum of the obtained liposomal formulations (Fig. 4), the L formulations exhibit an absorption peak at 220 nm due to the conjugated double bonds (Fig. 4A). Furosemide (Fig. 4A) showed peaks of maximum absorbance at 234, 273, and 343 nm, associated with its substituted aromatic system, consistent with previous reports [50]. The L:Fr formulation (Fig. 4B) shows UV–visible absorption peaks characteristic of Fr, with a bathochromic shift at 273 nm and a hypsochromic shift at 343 nm. These changes suggest alterations in the electronic environment of Furosemide upon interaction with the liposomal matrix. The bathochromic shift could be associated with stabilization of the excited state due to increased polarity or hydrogen-bond interactions.

In contrast, the hypsochromic shift could indicate partial localization of the molecule in a less polar environment within the lipid bilayer. These changes suggest alterations in the electronic environment of Furosemide upon interaction with the liposomal matrix. The 220 nm signal in L, integrated into the 234 nm peak, was not observed (Fig. 4A). Therefore, this behavior is consistent with Furosemide's amphiphilic nature, which allows it to distribute between the aqueous phase and the lipid membrane. Furthermore, interactions between the functional groups of Furosemide and the hydrophobic head groups or chains of the phospholipids could contribute to the observed spectral modifications.

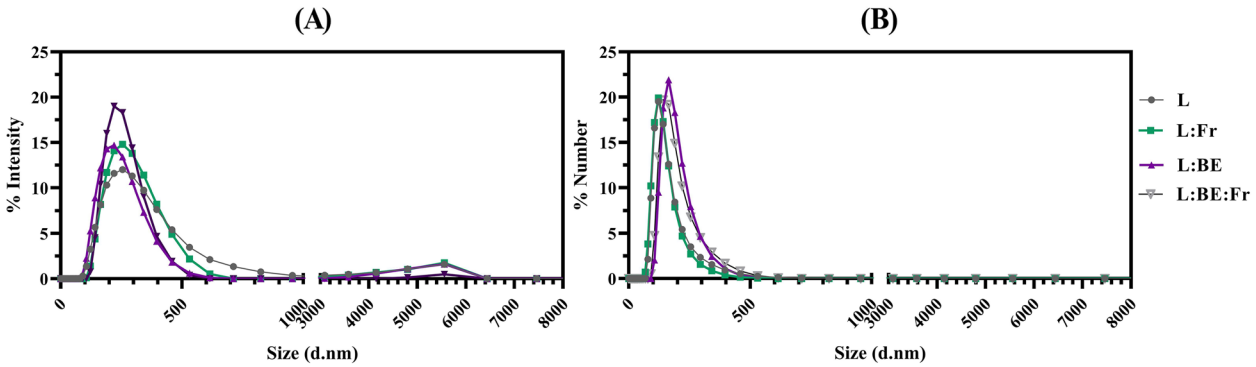

Fig. 3 Hydrodynamic size distribution of (**A**) Intensity percent, and (**B**) Number percent measured by dynamic light scattering of the obtained liposomal formulations

On the other hand, in both the L:BE and L:BE:Fr systems, only the blueberry extract band between 250 and 280 nm is observed (Fig. 4B). This finding could be explained by the broader band corresponding to the sum of the 273 nm peak, characterized by Fr, with a bathochromic shift. Consequently, this could be the first indication that BE interacts with liposomal components. The bathochromic shift could be associated with the stabilization of the excited state due to increased polarity or hydrogen bonding interactions. Based on the analysis performed and comparing the UV–visible spectra of L:BE:Fr and L:BE, it can be inferred that BE promotes the interaction of Fr with the lipid chains in the liposome interstitial. BE is in the liposomes' hydrophilic region, leading to lipid separation and contributing to Fr encapsulation. Taken together, these results support the existence of specific interactions of the components with the lipids.

In the fluorescence emission spectra, when excited at 280 nm, it was observed that in both the L:Fr and L:BE:Fr systems, there was no fluorescence emission in the 300–550 nm range, which could be attributed to quenching phenomena. These phenomena occur due to interactions between Fr and the lipid chains or between Fr and molecules in the blueberry extract. On the other hand, liposomes do not inherently fluoresce, so the fluorescence observed in the L control system may be due to scattered light incident on the nanometric liposomes. When excited at 300 nm, no fluorescence emission was observed in the 310–580 nm range for any formulations (L:BE and L:BE:Fr), indicating an interaction between the BE molecules and the lipids, between the BE and Fr molecules, or among them, leading to the lack of detection of fluorescence emission from the blueberry extract.

The FT-IR spectra of liposomal formulations are shown in Fig. 5. In all cases, a broad peak at 3300–3400 cm^{-1} is observed, corresponding to hydroxyl groups present in all formulations, originating from polyphenols in the BE, characteristic of anthocyanins, as well as from the lipids used to form the liposomes or from Furosemide (Fr). Comparison of the complete L:BE:Fr nanosystem with L:BE shows a spectrum like that of BE alone. Notably, a new peak appears at 2900 cm^{-1}, characteristic of methyl and methylene groups in lipids. According to the literature, CH_2 and CH_3 vibrations are expected at 2853 cm^{-1} and 2870 cm^{-1}, respectively, which are also observed in the IR spectrum of L. The absence of the peak at 1630 cm^{-1}, typically associated with conjugated double bonds in the aromatic rings of anthocyanins, suggests interactions between lipids and anthocyanins. Additionally, the peak at 1000 cm^{-1} can be attributed to C–O and C–C stretching vibrations typical of anthocyanins, indicating that the blueberry extract interacts with the liposome surface, with a fraction potentially encapsulated within the hydrophilic interior. Furosemide, in turn, appears to interact with the lipid bilayer.

For free Fr, the bands at 3340 cm^{-1} and 3250 cm^{-1} correspond to the stretching of hydroxyl (-OH) and amino (-NH) groups of the secondary amine. The band at 1676 cm^{-1} is assigned to carbonyl stretching (- C=O), indicative of the ketone moiety. The signal at 1556 cm^{-1} corresponds to C=C vibrations in the aromatic ring, while the band at 1340 cm^{-1} is likely due to S=O stretching of the sulfonamide group. Finally, the band at 1164 cm^{-1} corresponds to C–O vibrations, reflecting the presence of oxygen-containing functional groups, consistent with previous reports [51].

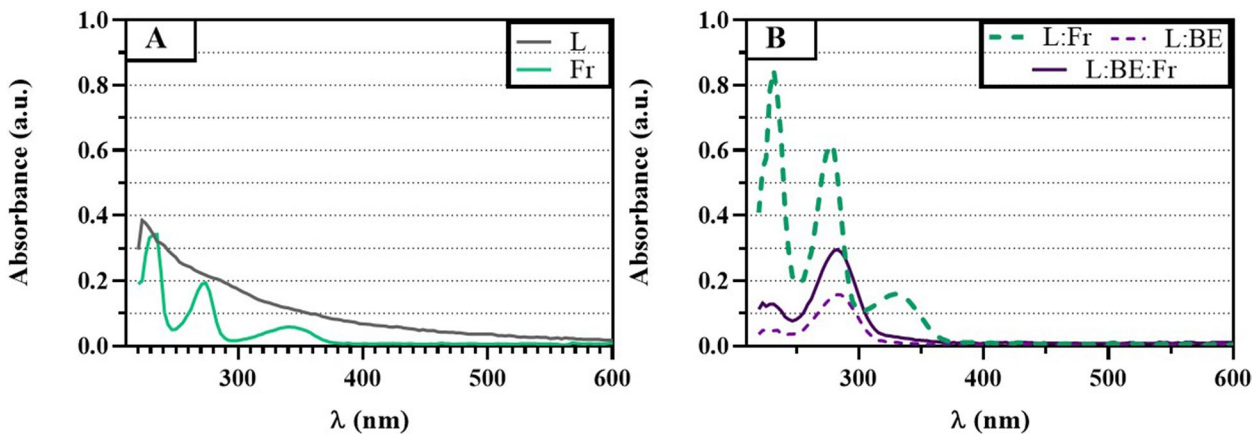

Fig. 4 UV–visible spectroscopy of liposomal formulations. Panel **A** shows the spectra of empty liposomal formulations (L) and Furosemide (Fr). Panel **B** displays the spectrum of formulations composed of liposomes in blueberry extract (L:BE), liposomes with Furosemide (L:Fr), and the complete formulation consisting of liposomes containing Furosemide in blueberry extract (L:BE:Fr)

In the L:Fr formulation, the peak at 2900 cm^{-1} associated with methyl/methylene groups is absent, whereas the peak at 1636 cm^{-1} remains, likely reflecting the keto groups of Furosemide. The increased absorbance at 3355 cm^{-1} suggests that a portion of Furosemide remains in solution, i.e., unencapsulated, while another fraction interacts with the apolar tails of the phospholipids in the bilayer.

Overall, the FT-IR analysis supports the conclusions drawn from UV–Vis spectroscopy, confirming that anthocyanins in the blueberry extract facilitate interactions between Furosemide and the lipids in the liposomal formulations.

The DPPH assay confirmed the antioxidant capacity of the free BE. However, when incorporated into liposomal formulations (Supplementary material), no antioxidant activity was detected under the tested conditions. The absence of detectable antioxidant activity in BE-loaded liposomes cannot be attributed solely to limited accessibility. In fact, given the IC50 of the free extract (~27 mg/mL) and considering the encapsulation efficiency, the effective concentration of BE available in the liposomal formulations is likely below this threshold, which could explain the lack of detectable activity under the tested conditions. In this regard, it has been reported that the antioxidant activity of compounds after liposomal encapsulation depends not only on their intrinsic chemical reactivity but also on their incorporation efficiency, localization within the vesicle, and interactions with the lipid membrane [52]. Furthermore, the compartmentalization of anthocyanins within the liposomes' aqueous core, along with the lipid bilayer acting as a diffusion barrier, significantly limits their interaction with the DPPH radical. This effect could be enhanced by interactions between anthocyanins and phospholipids, as shown in Fig. 5, potentially reducing their chemical reactivity and even confirming the L-BE interaction.

Moreover, the evaluation of antioxidant activity in dispersed or encapsulated systems is strongly influenced by partitioning phenomena, which may limit the accessibility of antioxidants to the reactive species [53]. Therefore, the absence of measurable antioxidant activity in liposomes does not necessarily indicate a loss of functionality, but rather reflects a combination of low effective concentration, physicochemical compartmentalization, and methodological limitations. Therefore, the DPPH assay, while suitable for free antioxidant compounds in homogeneous solutions, may be limited to liposomal formulations without considering compound release or accessibility. Similar studies have shown that antioxidant activity in liposomal systems may vary with experimental conditions and the extent of compound release from the carrier [54]. Taken together, these findings suggest that the absence of detectable antioxidant activity in BE-loaded liposomes under the present conditions does not necessarily indicate a loss of functionality but rather reflects methodological limitations and limited interaction between the encapsulated compounds and the DPPH radical.

Hemato-toxicological profile in bovine red blood cells

Hemolysis is damage to red blood cells that releases hemoglobin into the plasma [55]. In vivo hemolysis can lead to anemia, jaundice, and other adverse effects, underscoring the need to assess the hemolytic potential of all intravenously administered pharmaceutical products. Most studies of particle-induced hemolysis are assessed by spectroscopic detection of free plasma hemoglobin after incubation with blood. Hemocompatibility studies are commonly used as preliminary tools

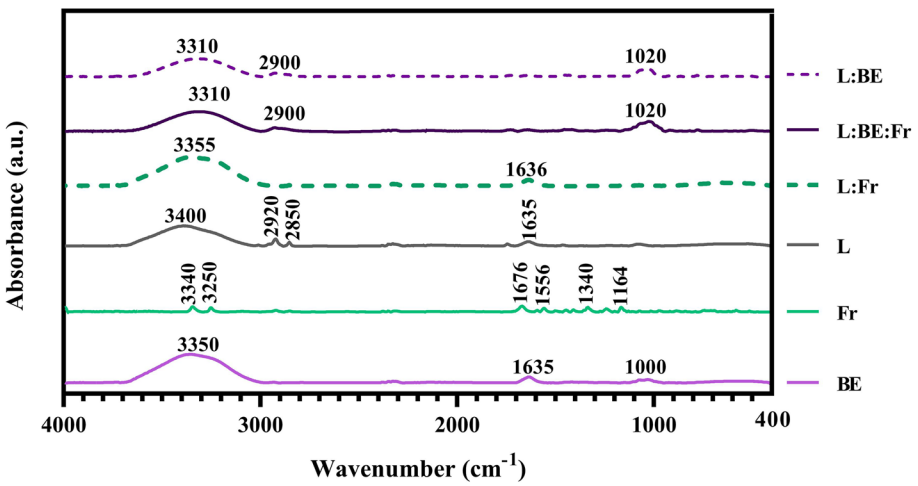

Fig. 5 FT-IR spectroscopy of liposomal formulations

in nanotoxicological assessment to evaluate interactions between nanomaterials and blood components [56]. Among these approaches, hemolysis assays provide a simple and sensitive method to assess potential damage to erythrocyte membranes caused by nanoparticle exposure. In the present study, bovine red blood cells were used as a biologically relevant model because the proposed formulation is intended for veterinary applications in cattle. Additionally, nanoparticles may influence erythrocyte aggregation, deformability, and membrane stability, which are key factors affecting hemorheological behavior and microcirculatory flow. Therefore, in the next section, hemocompatibility and hemorheological analyses were also performed to obtain preliminary information on the potential interaction of liposomal formulations with bovine blood cells.

Figure 6 shows the percentage of released hemoglobin normalized to CTR + from the treatments tested 24 h post-incubation. In all cases, the hemolysis percentage remained below 2% across the tested concentration range. According to commonly accepted criteria for hemocompatibility assessment, materials inducing hemolysis below 5% are generally classified as non-hemolytic and considered compatible with erythrocyte membranes [55]. Therefore, the results of this study suggest that the evaluated liposomal formulations do not induce significant erythrocyte membrane damage under the tested conditions. Figure 6A shows the most concentrated solutions of each formulation and its components, while graphs 6B, 6C, and 6D correspond to these serial dilutions. When comparing the mean values of each sample with the negative control (CTR −), no statistically significant differences were observed at the conventional significance level ($p < 0.05$). However, in the most concentrated samples (Fig. 6A), a tendency toward lower hemolysis was observed for L, L:BE, and L:BE:Fr relative to the control ($p < 0.1$). Because this threshold does not meet the conventional significance level, these results were interpreted as indicative trends rather than statistically significant differences. Furthermore, hemolysis percentages did not differ significantly among the tested formulations. Overall, hemoglobin release across the

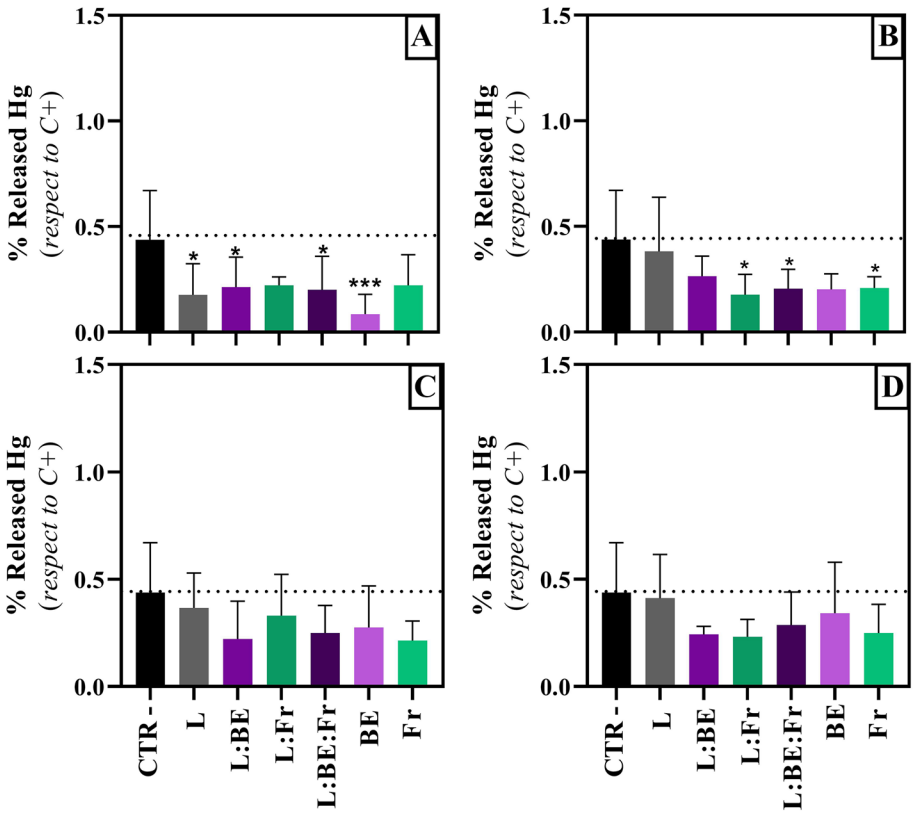

Fig. 6 Percentage of hemoglobin (Hg) released 24 h post-incubation of the different treatments relative to CTR + (n = 6). The CTR- sample corresponds to the negative control (bRBCs incubated with PBS at physiological pH). The treatment formulations L:(BE):[Fr] is shown as follows: **A** displays solution concentrations of 25 mM:(26.6 mg/ml):[1.5 mM]; **B** shows concentrations of 12.5 mM:(13.5 mg/ml):[0.7 mM]; **C** exhibits concentrations of 6.2 mM:(6.7 mg/ml):[0.4 mM]; and **D** displays concentrations of 3.1 mM:(3.4 mg/ml):[0.2 mM]. Statistical analysis was performed using one-way ANOVA followed by Dunnett's post hoc test for comparisons against control. Symbols indicate statistical significance relative to the control (*$p < 0.05$, and ***$p < 0.001$)

entire concentration range remained well below the 5% threshold, suggesting that the liposomal formulations exhibit good hemocompatibility and do not induce significant erythrocyte membrane damage under the tested conditions.

Microscopy of bRBC smear after treatment

Erythrocytes are the most numerous cells in the blood. These cells exhibit a typical biconcave shape characteristic of mammalian red blood cells. In cattle, anisocytosis is also observed, corresponding to the different sizes typical of bovine red blood cells [57] and their characteristic morphological alteration, autoagglutination [58].

Figure 7 shows optical microscopy images of bovine red blood cells (bRBCs) treated with the highest concentrations used in the hemocompatibility assays. Samples that exhibited non-hemolytic behavior were selected for qualitative analysis. A lower apparent cell density was observed in samples treated with free furosemide compared to the negative control and other treatments. However, this observation must be interpreted with caution. The furosemide stock solution contained ethanol, resulting in a final concentration of approximately 5% in the assay medium. At this concentration, ethanol may affect erythrocyte membrane properties and smear distribution, potentially contributing to the observed differences. Since a matched vehicle control containing the same ethanol concentration was not included, it is not possible to distinguish between solvent-related effects and those attributable to furosemide. Therefore, no specific conclusions can be drawn regarding the direct effect of furosemide on erythrocyte morphology based on these observations. Therefore, bRBCs treated BE at its IC50, L:BE, L:Fr, and L:BE:Fr do not show changes compared to the negative control while maintaining their typical agglutination behavior.

Furthermore, a reduction in anisocytosis is observed in the microphotographs of cells exposed to liposomal formulations. This reduction could be due to the liposomes' composition, which is phosphatidylcholine. According to Cyboran-Mikołajczyk et al., (2021), who studied the impact of lecithin liposomes on red blood cells after their interaction, they demonstrated that these significantly influence membrane potential, stiffness, and the shape of RBC, leading to a decrease in the number of stomatocytes and a lower proportion of cells with irregular shapes, thus increasing erythrocyte survival time [59]. Therefore, this could indicate that Fr and BE in the phosphatidylcholine liposomal formulation may benefit erythrocyte survival time. Moreover, those above could indicate an improvement in the quality of life of livestock.

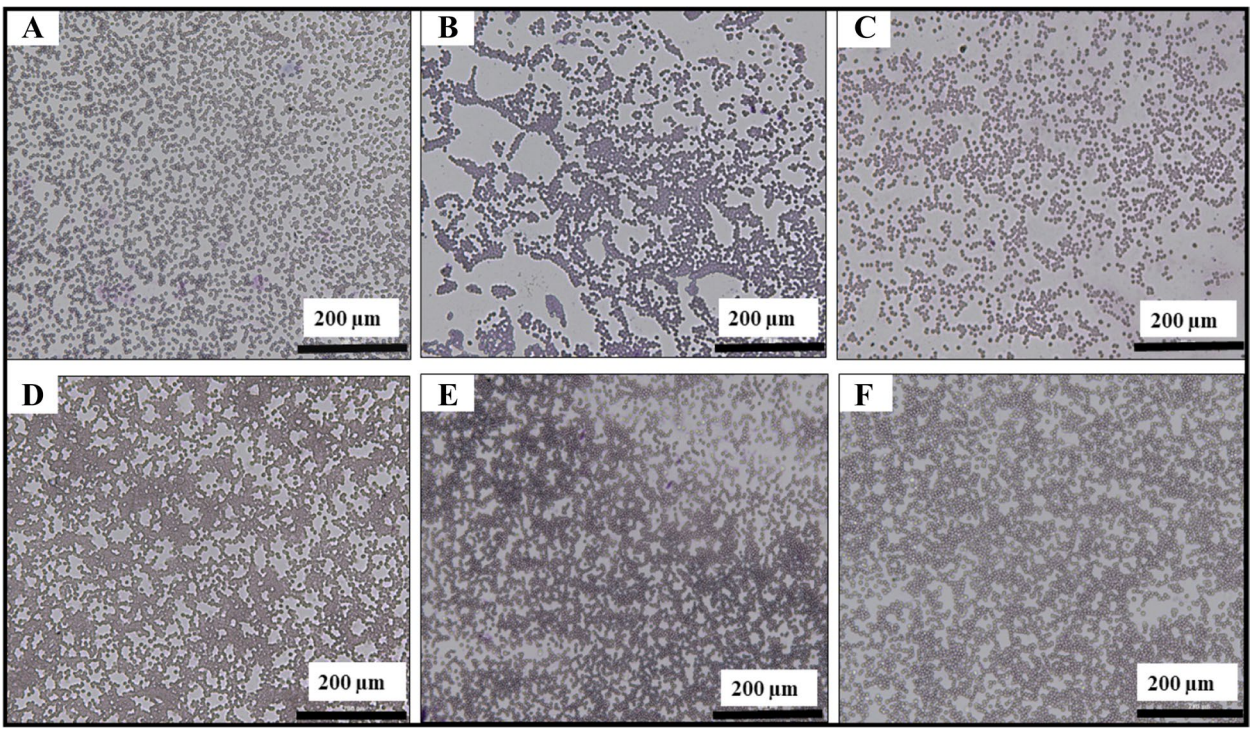

Fig. 7 Microscopy of bovine red blood cells, stained with Giemsa, after treatment with BE (**A**); Furosemide (**B**); empty liposomes (**C**); empty liposomes with BE (**D**); liposomes containing Furosemide (**E**); and liposomes with Furosemide and BE (**F**)

Table 3 Erythrocyte viscoelastic parameters obtained with the Erythrocyte Rheometer: elastic modulus (μ), deformability index (DI), and surface viscosity (ηm) of the membrane of bRBCs treated with the formulations. Statistical analysis was performed using one-way ANOVA. Statistical analysis performed was * corresponds to a *p*-value < 0.05 compared with respect to the control ($n = 5$)

Samples	μ 10^{-6} N/m	ID	ηm 10^{-7} N.s/m
Control	4.483 ± 0.041	0.593 ± 0.003	1.79 ± 0.94
L	4.410 ± 0.058	0.600 ± 0.005	1.28 ± 0.33
L:BE	4.403 ± 0.043*	0.601 ± 0.004*	2.18 ± 0.87
L:Fr	4.445 ± 0.026	0.597 ± 0.002	1.58 ± 0.61
L:BE:Fr	4.463 ± 0.052	0.595 ± 0.005	2.50 ± 0.03
BE	4.447 ± 0.027	0.597 ± 0.002	1.54 ± 0.64

Rheological properties and morphological studies of bRBC

Table 3 presents the viscoelastic parameters of the bRBC samples treated with the different formulation media, with PBS as the control sample. Figure 8 shows an example of the microscopic images obtained from the same bRBC samples suspended in autologous plasma at a concentration of 0.25%.

In Table 3, viscoelastic parameters of erythrocytes from L, L:Fr, L:BE:Fr, and BE show no significant alterations compared with the control. Whereas the treatment with L:BE induces a slight decrease in the membrane elasticity modulus and an increase in the deformability index of bRBCs. This result indicates that this formulation slightly decreased the stiffness of the bRBCs, making them more deformable. Although these variations are statistically significant, they are relatively small (less than 2%) compared to the control values.

Figure 7 shows photomicrographs of bRBCs in a smear after fixation to glass and staining with Giemsa. However, in such cases, the erythrocyte crenation by the glass effect could occur [60, 61]. This phenomenon consists of alterations in the erythrocyte membrane adhered to the glass by which fine and numerous evenly distributed spicules are generated, giving the erythrocyte the echinocyte shape. For these reasons, microscopic images in Fig. 8 were registered from treated bRBC suspended in autologous plasma. Qualitative analysis of these images shows no significant morphological alterations compared to the control [62]. Consequently, the analysis of erythrocyte morphology and mechanical properties indicates that all the additives analyzed in this work are hemorheologically compatible with the bRBC.

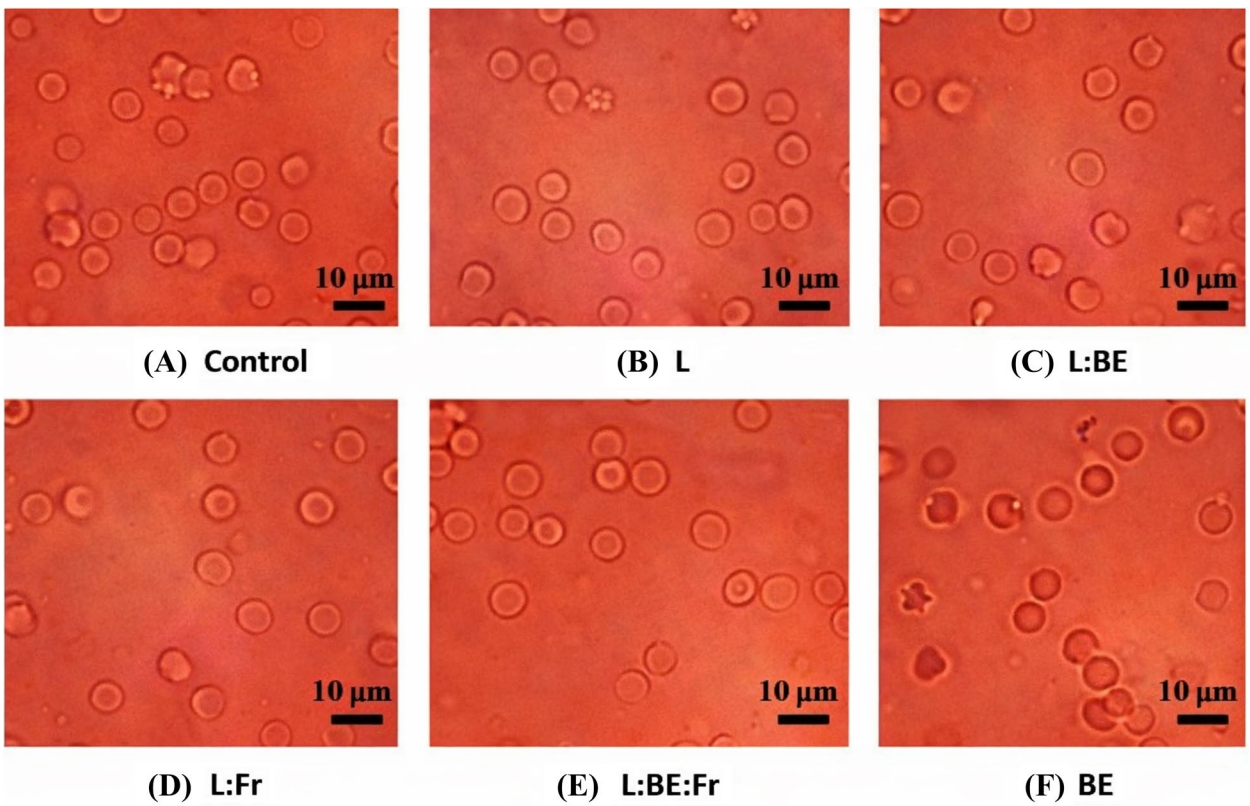

Fig. 8 Microscopic images of bRBC control (**a**) and treated with L (**b**), L:BE (**c**), L:Fr (**d**), L:BE:Fr (**e**), and BE (**f**). Images were obtained using an inverted microscope from bRBC suspended in autologous plasma at 0.25% v/v

Conclusions

Liposomal formulations incorporating Furosemide (Fr) and an anthocyanin-rich blueberry extract (BE) were developed and physicochemically characterized. The systems exhibited nanoscale size distribution, acceptable polydispersity, and negative zeta potential, consistent with the formation of vesicles containing SPC and stearic acid.

Encapsulation efficiency analysis showed effective loading for single-compound systems, particularly for BE, while Fr exhibited moderate incorporation. However, in the co-loaded formulation, a marked reduction in encapsulation efficiency was observed, especially for Fr (0.8%), indicating limited co-loading under the conditions studied. These results suggest that their physicochemical properties constrain the simultaneous incorporation of both compounds and require further optimization of formulation parameters.

The blueberry extract demonstrated antioxidant activity in its free form. In contrast, no detectable activity was observed in liposomal systems under the evaluated conditions, likely due to limited accessibility and reduced effective concentration of the encapsulated compounds.

Hemocompatibility studies showed that the formulations did not induce significant hemolysis in bovine red blood cells, and hemorheological analyses indicated no adverse effects on erythrocyte behavior, supporting their compatibility with blood components under the tested conditions.

Overall, these findings indicate that liposomal systems are suitable for the incorporation and evaluation of BE and for studying interactions with erythrocytes. However, efficient co-encapsulation of Furosemide was not achieved in the present formulation, highlighting the need for further optimization to enable effective co-delivery in future applications.

Supplementary Information

The online version contains supplementary material available at https://doi.org/10.1186/s44331-026-00018-6.

Supplementary Material 1.

Acknowledgements

Victoria Judurcha acknowledges the student fellowship from Consejo Interuniversitario Nacional (EVC-CIN). David Ybarra and Ayelen Sosa are grateful for the postdoctoral fellowships from Consejo Nacional de Investigaciones Científicas y Técnicas (CONICET). Silvia del Valle Alonso is a member of CONICET. Analía I. Alet, Bibiana D. Riquelme, Horacio V. Castellini are researchers of the Universidad Nacional de Rosario.

Authors' contributions

Victoria Judurcha: methodology, formal analysis, data curation, writing. Ayelen M. Sosa methodology, formal analysis, writing Analía I. Alet writing and formal analysis. Marcus V. Batista da Silva sample preparation Horacio V. Castellini formal analysis, statistics analysis Bibiana D. Riquelme formal analysis, statistics analysis, writing—review. Silvia del V. Alonso Conceptualization, Methodology, Validation and Investigation, Project Administration, Funding Acquisition, Formal Analysis, Review—Editing. David Emanuel Ybarra conceptualization, methodology, formal analysis, data curation, validation, writing—review.

Funding

This research was supported by the Universidad Nacional de Quilmes, PUNQ BIONATLP Res. CS. #149/24. The financial support is gratefully acknowledged.

Data availability

No datasets were generated or analysed during the current study.

Declarations

Ethics approval and consent to participate

This study did not involve live animals or in vivo experimentation. Bovine blood samples were obtained post mortem from animals slaughtered for human consumption at a licensed abattoir (Frigorífico Cooperativa Subpga, B1884HEH, Berazategui Oeste, Argentina), as a by-product of the food industry. Blood collection was performed within 2 h post mortem in accordance with standard industrial procedures.

No animals were handled or sacrificed specifically for research purposes. Therefore, the study is not considered an animal experiment under applicable regulations and does not fall within the scope of ARRIVE guidelines. According to institutional guidelines, studies using post-mortem material from commercial sources do not require formal ethical approval.

Competing interests

The authors declare no competing interests.

Author details

[1]Laboratorio de Bio-Nanotecnología, Departamento de Ciencia y Tecnología, Universidad Nacional de Quilmes, B1876BXD Bernal, Buenos Aires, Argentina. [2]Grupo de Biología Estructural y Biotecnología (GBEyB), Instituto Multidisciplinario de Biología Celular (IMBICE), CONICET – CCT La Plata, B1900 La Plata, Bs As, Argentina. [3]Facultad Cs. Bioquímicas y Farmacéuticas, Universidad Nacional de Rosario, Rosario, Argentina. [4]Facultad Cs. Exactas Ingeniería y Agrimensura, Universidad Nacional de Rosario, Rosario, Argentina. [5]Consejo de Investigaciones de La Universidad Nacional de Rosario, Rosario, Argentina. [6]Grupo de Física Biomédica, IFIR (CONICET-UNR), Rosario, Argentina. [7]Laboratorio de Nanosistemas de Aplicación Biotecnológica (LANSAB), Universidad Nacional de Hurlingham, CP 1688 Hurlingham, Buenos Aires, Argentina. [8]Comisión Nacional de Investigaciones Científicas y Técnicas (CONICET), Buenos Aires, Argentina. [9]Laboratorio de Investigación en Funcionalidad y Tecnología de Alimentos (LIFTA), Departamento de Ciencia y Tecnología, Universidad Nacional de Quilmes, Bernal, Argentina. [10]Consejo de Investigaciones UNR (CIUNR), Rosario, Argentina.

Received: 13 February 2026 Revised: 20 April 2026 Accepted: 23 May 2026
Published online: 01 June 2026

References

1. von Keyserlingk MAG, Rushen J, de Passillé AM, Weary DM. Invited review: the welfare of dairy cattle—key concepts and the role of science. J Dairy Sci. 2009;92(9):4101–11. https://doi.org/10.3168/jds.2009-2326.
2. Kumar A, Mandal RSK, Bhatt S, Kumar A. Physiological edema. In: Periparturient diseases of cattle. John Wiley & Sons, Ltd; 2024. p. 331–8. https://doi.org/10.1002/9781394204007.ch30.
3. Okkema C, Eilertson K, Grandin T. Effects of udder edema on parlor behavior in first- and second-lactation Holstein dairy cows. J Dairy Sci. 2023;106(11):7924–31. https://doi.org/10.3168/jds.2022-22761.
4. Morrison EI, DeVries TJ, LeBlanc SJ. Short communication: associations of udder edema with health, milk yield, and reproduction in dairy cows in early lactation. J Dairy Sci. 2018;101(10):9521–6. https://doi.org/10.3168/jds.2018-14539.
5. González Salas R, Vidal del Río MM. Bovine mastitis and milk quality: a challenge for human health. Univ Soc. 2022;13(S1):89–96. Available from: https://rus.ucf.edu.cu/index.php/rus/article/view/2013.

6. Stanker LH, Muldoon MT, Buckley SA, Braswell C, Kamps-Holtzapple C, Beier RC. Development of a monoclonal antibody-based immunoassay to detect Furosemide in cow's milk. J Agric Food Chem. 1996;44(8):2455–9. https://doi.org/10.1021/jf9503624.
7. Nkansah P, Antipas A, Lu Y, Varma M, Rotter C, Rago B, et al. Development and evaluation of novel solid nanodispersion system for oral delivery of poorly water-soluble drugs. J Control Release. 2013;169(1):150–61. https://doi.org/10.1016/j.jconrel.2013.03.032.
8. Zhang MQ, Heirbaut S, Hertogs K, Girma M, Geerinckx K, Stevens E, et al. Periparturient oxidative and inflammatory status and their relation to energy metabolism and performance in transition dairy cows. J Dairy Sci. 2025;108(12):13872–89. https://doi.org/10.3168/jds.2025-26798.
9. Ayemele AG, Tilahun M, Lingling S, Elsaadawy SA, Guo Z, Zhao G, et al. Oxidative stress in dairy cows: insights into the mechanistic mode of actions and mitigating strategies. Antioxidants. 2021. https://doi.org/10.3390/antiox10121918.
10. García Bacallao L, García Gómez LV, Rojo Domínguez DM, Sánchez García E. Plantas con propiedades antioxidantes. Rev Cubana Invest Bioméd. 2001;20(3):231–235. Available from: http://scielo.sld.cu/scielo.php?script=sci_arttext&pid=S0864-03002001000300011&lng=es.
11. Vilaplana Batalla M. Antioxidantes presentes en los alimentos: vitaminas, minerales y suplementos. Offarm. 2007;26:79–86. ISSN-e 1578–1569. Available from: https://dialnet.unirioja.es/servlet/articulo?codigo=5324583.
12. Garzón GA. Anthocyanins As Natural Colorants And Bioactive Compounds: A Review. Acta Biológica Colombiana. 2008. 13(3):27–36. Available from: http://www.scielo.org.co/scielo.php?script=sci_abstract&pid=S0120-548X2008000300002&lng=en&nrm=iso&tlng=es.
13. Salehi B, Sharifi-Rad J, Cappellini F, Reiner Ž, Zorzan D, Imran M, et al. The therapeutic potential of anthocyanins: current approaches based on their molecular mechanism of action. Front Pharmacol. 2020. https://doi.org/10.3389/fphar.2020.01300.
14. Ayvaz H, Cabaroglu T, Akyildiz A, Pala CU, Temizkan R, Ağçam E, et al. Anthocyanins: metabolic digestion, bioavailability, therapeutic effects, current pharmaceutical/industrial use, and innovation potential. Antioxidants Basel. 2022. https://doi.org/10.3390/antiox12010048.
15. Giampieri F, Alvarez-Suarez JM, Mazzoni L, Forbes-Hernandez TY, Gasparrini M, Gonzàlez-Paramàs AM, et al. An anthocyanin-rich strawberry extract protects against oxidative stress damage and improves mitochondrial functionality in human dermal fibroblasts exposed to an oxidizing agent. Food Funct. 2014;5(8):1939–48. https://doi.org/10.1039/C4FO00048J.
16. Palungwachira P, Tancharoen S, Dararat P, Nararatwanchai T. Anthocyanins isolated from *Oryza sativa* L. protect dermal fibroblasts from hydrogen peroxide-induced cell death. J Nat Sci Biol Med. 2020;11(1):45. https://doi.org/10.4103/jnsbm.JNSBM_171_19.
17. Munir N, Gulzar W, Abideen Z, Hancock JT, El-Keblawy A, Radicetti E. Nanotechnology improves disease resistance in plants for food security: applications and challenges. Biocatal Agric Biotechnol. 2023;51:102781. https://doi.org/10.1016/j.bcab.2023.102781.
18. Takeshita V, Preisler AC, Munhoz-Garcia GV, de Oliveira FF, Milagres JS, Rodrigues JS, et al. The green horizon of agricultural nanotechnology: a pathway for truly sustainable pesticide formulations. Sustain Mater Technol. 2025;46:e01756. https://doi.org/10.1016/j.susmat.2025.e01756.
19. Maja L, Željko K, Mateja P. Sustainable technologies for liposome preparation. J Supercrit Fluids. 2020;165:104984. https://doi.org/10.1016/j.supflu.2020.104984.
20. Apolinário AC, Hauschke L, Nunes JR, Lopes LB. Lipid nanovesicles for biomedical applications: 'what is in a name'? Prog Lipid Res. 2021;82:101096. https://doi.org/10.1016/j.plipres.2021.101096.
21. Chacko IA, Ghate VM, Dsouza L, Lewis SA. Lipid vesicles: a versatile drug delivery platform for dermal and transdermal applications. Colloids Surf B Biointerfaces. 2020;195:111262. https://doi.org/10.1016/j.colsurfb.2020.111262.
22. Guimarães D, Cavaco-Paulo A, Nogueira E. Design of liposomes as drug delivery system for therapeutic applications. Int J Pharm. 2021;601:120571. https://doi.org/10.1016/j.ijpharm.2021.120571.
23. Sebaaly C, Greige-Gerges H, Stainmesse S, Fessi H, Charcosset C. Effect of composition, hydrogenation of phospholipids and lyophilization on the characteristics of eugenol-loaded liposomes prepared by ethanol injection method. Food Biosci. 2016;15:1–10. https://doi.org/10.1016/j.fbio.2016.04.005.
24. Zhang F, Mao J, Tian G, Jiang H, Jin Q. Preparation and characterization of furosemide solid dispersion with enhanced solubility and bioavailability. AAPS PharmSciTech. 2022;23(1):65. https://doi.org/10.1208/s12249-022-02208-w.
25. Mohammed-Kadhum MF, Hameed GS. Development and characterization of furosemide-loaded binary amorphous solid dispersion to enhance solubility and dissolution for pediatric oral administration. Pharmacia. 2025;72:1–19. https://doi.org/10.3897/pharmacia.72.e156784.
26. Wang L, Lan W, Chen D. Blueberry (*Vaccinium* spp.) anthocyanins and their functions, stability, bioavailability, and applications. Foods. 2024. https://doi.org/10.3390/foods13172851.
27. Xing H, Hwang K, Lu Y. Recent developments of liposomes as nanocarriers for theranostic applications. Theranostics. 2016;6:1336–52. https://doi.org/10.7150/thno.15464.
28. Abbasi H, Kouchak M, Mirveis Z, Hajipour F, Khodarahmi M, Rahbar N, et al. What We Need to Know about Liposomes as Drug Nanocarriers: An Updated Review. Adv Pharm Bull. 2023;13(1):7–23. https://doi.org/10.34172/apb.2023.009.
29. Jiang Y, Li W, Wang Z, Lu J. Lipid-based nanotechnology: liposome. Pharmaceutics. 2023. https://doi.org/10.3390/pharmaceutics16010034.
30. Chen HW, Chen SD, Wu HT, Cheng CH, Chiou CS, Chen WT. Improvement in curcumin's stability and release by formulation in flexible nanoliposomes. Nanomaterials. 2024. https://doi.org/10.3390/nano14221836.
31. Kim EM, Jeong HJ. Liposomes: biomedical applications. Chonnam Med J. 2021;57(1):27–35. https://doi.org/10.4068/cmj.2021.57.1.27.
32. Ramli NA, Ali N, Hamzah S, Yatim NI. Physicochemical characteristics of liposome encapsulation of stingless bees' propolis. Heliyon. 2021. https://doi.org/10.1016/j.heliyon.2021.e06649.
33. Giordano Maffioli N. Solid lipid microparticles as carriers of *Vaccinium myrtillus* and *Schinus molle* Linn additives for food application. FSN. 2023;9(3):1–8. https://doi.org/10.24966/FSN-1076/100162.
34. Franceschinis G, Beverina M, Corleto M, Sosa AM, Lillo C, Arias Casará L, et al. Green-synthesized silver nanoparticles using *Aloe maculata* extract as antibacterial agent for potential topical application. OpenNano. 2023;12:100148. https://doi.org/10.1016/j.onano.2023.100148.
35. Kamel EM, Mahmoud AM, Ahmed SA, Lamsabhi AM. A phytochemical and computational study on flavonoids isolated from *Trifolium resupinatum* L. and their novel hepatoprotective activity. Food Funct. 2016;7(4):2094–106. https://doi.org/10.1039/C6FO00194G.
36. Marsanasco M, Piotrkowski B, Calabró V, del Valle Alonso S, Chiaramoni NS. Bioactive constituents in liposomes incorporated in orange juice as new functional food: thermal stability, rheological and organoleptic properties. J Food Sci Technol. 2015;52(12):7828–38. https://doi.org/10.1007/s13197-015-1924-y.
37. Fry DW, White JC, Goldman ID. Rapid separation of low molecular weight solutes from liposomes without dilution. Anal Biochem. 1978;90(2):809–15. https://doi.org/10.1016/0003-2697(78)90172-0.
38. Temprana CF, Prieto MJ, Igartúa DE, Femia AL, Amor MS, Alonso S. Diacetylenic lipids in the design of stable lipopolymers able to complex and protect plasmid DNA. PLOS ONE. 2017;12(10):e0186194. https://doi.org/10.1371/journal.pone.0186194.
39. Londero CM, D'Arrigo M, Riquelme BD. Optimización del medio de suspensión para la observación de glóbulos rojos humanos frescos con microscopios ópticos. Acta Microscopica. 2016;25(3):151–156. Available from: https://d1wqtxts1xzle7.cloudfront.net/112899613/132-Article_Text-455-1-10-20200707-libre.pdf.
40. Fontana AB, Lerda N, Delannoy MM, Alessi AC, Riquelme BD. Técnica de cuantificación de la agregación eritrocitaria por análisis digital de imágenes. Acta bioquímica clínica latinoamericana. 2012; 46(1):47–52. Available from: http://www.scielo.org.ar/scielo.php?script=sci_abstract&pid=S0325-29572012000100007&lng=es&nrm=iso&tlng=es.
41. Alet AI, Basso S, Delannoy M, Alet NA, D'Arrigo M, Castellini HV, et al. Innovative parameters obtained for digital analysis of microscopic images to evaluate in vitro hemorheological action of anesthetics. In: Biophotonics South America. SPIE; 2015. p. 187–92. https://doi.org/10.1117/12.2180791.
42. Alet A, Basso S, Castellini H, Delannoy M, Nicolás A, D'Arrigo M, et al. Hemorheological in vitro action of propofol on erythrocytes from healthy donors and diabetic patients. Clin Hemorheol Microcirc. 2016. https://doi.org/10.3233/CH-162054.

43. Batista da Silva MV, Castellini HV, Alet NA, Riquelme BD, Alet AI. Erythrocyte rheology under anesthesia: insights from glycated and non-glycated red blood cells. Microvascular Research. 2026;164:104900. https://doi.org/10.1016/j.mvr.2025.104900.
44. Porini S, Riquelme BD, Castellini HV, Detarsio G, Aresi A, Manzelli N, et al. Protective effects of two standard preservation media on irradiated erythrocytes under storage conditions: A rheological comparative evaluation. Series on Biomechanics. 2024. Available from: http://jsb.imbm.bas.bg/page/en/details.php?article_id=808.
45. Arencibia JA, Rodríguez D, Casariego A, García MA. OPTIMIZACIÓN DE LA EXTRACCIÓN DE ANTOCIANINAS A PARTIR DE MANZANA MALAYA (Syzygium malaccense). Revista de Ciencias Farmacéuticas y Alimentarias. 2018; 4(1):1. Available from: https://revistas.uh.cu/rcfa/article/view/4209.
46. Welch CR, Wu Q, Simon JE. Recent Advances in Anthocyanin Analysis and Characterization. Current Analytical Chemistry. 2008;4(2):75–101. Available from: https://www.ingentacaonnect.com/content/ben/cac/2008/00000004/00000002/art00001.
47. Bartosz G, Grzesik-Pietrasiewicz M, Sadowska-Bartosz I. Fluorescent products of anthocyanidin and anthocyanin oxidation. J Agric Food Chem. 2020;68(43):12019–27. https://doi.org/10.1021/acs.jafc.0c04755.
48. Bahramabadi R, Hakimi H, Saljooqi A, Barani M, Razmjoue D, Zare-Bidaki M, et al. The essential oil of rocket seeds maintains its antibacterial effects after encapsulation in nanoliposomes. J Herb Med. 2024;47:100924. https://doi.org/10.1016/j.hermed.2024.100924.
49. Ali Dheyab M, Abdul Aziz A, Jameel MS, MoradiKhaniabadi P, Oglat AA. Rapid sonochemically-assisted synthesis of highly stable gold nanoparticles as computed tomography contrast agents. Appl Sci. 2020;10(20):7020. https://doi.org/10.3390/app10207020.
50. Mangal G, Dhobale S. Development of UV spectrophotometric methods for estimation of furosemide in bulk and tablet dosage forms. Int J Adv Pharma. 2016;5:160–70.
51. Sadr M, Nabipour H. Preparation and identification of furosemide nanoparticles. J Basic Appl Sci Res. 2013;3(2s):666–70.
52. Tan C, Xue J, Abbas S, Feng B, Zhang X, Xia S. Liposome as a delivery system for carotenoids: comparative antioxidant activity of carotenoids as measured by ferric reducing antioxidant power, DPPH assay and lipid peroxidation. J Agric Food Chem. 2014;62(28):6726–35. https://doi.org/10.1021/jf405622f.
53. Tsotsou GE, Paraskevopoulou PE. An extraction-free, smartphone-based approach for measuring the antioxidant capacity of emulsions using a paper-based DPPH assay. Microchem J. 2024;207:111792. https://doi.org/10.1016/j.microc.2024.111792.
54. Xu T, Zhang J, Jin R, Cheng R, Wang X, Yuan C, et al. Physicochemical properties, antioxidant activities and in vitro sustained release behaviour of co-encapsulated liposomes as vehicle for vitamin E and β-carotene. J Sci Food Agric. 2022;102(13):5759–67. https://doi.org/10.1002/jsfa.11925.
55. Neun BW, Dobrovolskaia MA. Method for analysis of nanoparticle hemolytic properties in vitro. In: McNeil SE, editor. Characterization of Nanoparticles Intended for Drug Delivery. Totowa: Humana Press; 2011. p. 215–224. https://doi.org/10.1007/978-1-60327-198-1_23.
56. Dobrovolskaia MA, Clogston JD, Neun BW, Hall JB, Patri AK, McNeil SE. Method for analysis of nanoparticle hemolytic properties In Vitro. Nano Lett. 2008;8(8):2180–7. https://doi.org/10.1021/nl0805615.
57. Sun PL, Jeffery U. Effect of dilution of canine blood samples on the specificity of saline agglutination tests for immune-mediated hemolysis. J Vet Intern Med. 2020;34(6):2374–83. https://doi.org/10.1111/jvim.15945.
58. Willard MD, Tvedten H, Turnwald GH. Diagnóstico clinico patológico práctico. En los pequeños animales. In: Diagnóstico clinico patológico práctico. En los pequeños animales. P. 428. Available from: https://pesquisa.bvsalud.org/portal/resource/pt/biblio-1202883.
59. Cyboran-Mikołajczyk S, Sareło P, Pasławski R, Pasławska U, Przybyło M, Nowak K, et al. Impact of liposomal drug formulations on the RBCs shape, transmembrane potential, and mechanical properties. Int J Mol Sci. 2021;22(4):4. https://doi.org/10.3390/ijms22041710.
60. Londero CM, D'Arrigo M, Riquelme BD. Optimización del medio de suspensión para la observación de glóbulos rojos humanos frescos con microscopios ópticos. Acta Microscopica. 2016;25(3):151–156. Available from: https://acta-microscopica.org/acta/article/view/132.
61. Mancilla Canales MA, Londero CM, Riquelme BD, Korol A. Identificación de equinocitos por análisis digital de imágenes microscópicas: optimización mediante transformada wavelet. CONICET repository. 2018. Available from: https://ri.conicet.gov.ar/handle/11336/95797.
62. Mascaro Grosso H, Buszniez P, Riquelme BD. Hemocompatibility and hemorheological activity of aqueous extracts from *Phyllanthus sellowianus*: effects on in vitro glycated erythrocytes. J Herb Med. 2024;48:100945. https://doi.org/10.1016/j.hermed.2024.100945.

Publisher's Note